

 Open access • Journal Article • DOI:10.1115/1.4026171

The Strength of High-Temperature Ag–In Joints Produced Between Copper by Fluxless Low-Temperature Processes — [Source link](#)

Yuan-Yun Wu, Chin C. Lee

Institutions: University of California, Irvine

Published on: 01 Mar 2014 - Journal of Electronic Packaging (American Society of Mechanical Engineers)

Topics: Copper and Scanning electron microscope

Related papers:

- [Development of Cu-Ag pastes for high temperature sustainable bonding](#)
- [Development of nanocomposite pastes for low-temperature low-pressure bonding](#)
- [Design of high strength Cu alloy interlayer for mechanical bonding Ti to steel and characterization of their tri-layered clad](#)
- [Fluxless Bonding of Ni-P/Cu Plated Al Alloy and Cu Alloy with Lead-Free Sn-Cu Foil](#)
- [Low-Resistance and high-Strength Copper Direct Bonding in no-Vacuum Ambient Using Highly \(111\)-Oriented Nano-Twinned Copper](#)

Share this paper:    

View more about this paper here: <https://typeset.io/papers/the-strength-of-high-temperature-ag-in-joints-produced-5go0pq9vrw>

UC Irvine

UC Irvine Previously Published Works

Title

The strength of high-temperature ag-in joints produced between copper by fluxless low-temperature processes

Permalink

<https://escholarship.org/uc/item/0mv7k4xd>

Journal

Journal of Electronic Packaging, Transactions of the ASME, 136(1)

ISSN

1043-7398

Authors

Wu, YY
Lee, CC

Publication Date

2014

DOI

10.1115/1.4026171

Peer reviewed

The Strength of High-Temperature Ag–In Joints Produced Between Copper by Fluxless Low-Temperature Processes

Yuan-Yun Wu¹

Electrical Engineering and Computer Science,
Materials and Manufacturing Technology,
University of California,
2226 Engineering Gateway Building,
Irvine, CA 92697-2660
e-mail: yuanyunw@uci.edu

Chin C. Lee

Electrical Engineering and Computer Science,
Materials and Manufacturing Technology,
University of California,
2226 Engineering Gateway Building,
Irvine, CA 92697-2660

Two copper (Cu) substrates were bonded using silver (Ag) and indium (In) and annealed at 200–250 °C to convert the joints into the solid solution (Ag) for enhanced strength and ductility. Cu–Cu pair was chosen so that the samples break in the joint during shear test. The upper Cu was electroplated with 15 μm Ag. The lower Cu was plated with 15 μm Ag, followed by In and 0.1 μm Ag to inhibit indium oxidation. Two designs were implemented, using 8 μm and 5 μm In, respectively. The Cu substrates were bonded at 180 °C in 100 mTorr vacuum without flux. Afterwards, samples were annealed at 200 °C for 1000 h (first design) and at 250 °C for 350 h (second design), respectively. Scanning electron microscope with energy dispersive X-ray analysis (SEM and EDX) results indicate that the joint of the first design is an alloy of mostly (Ag) with micron-size Ag₂In and (ζ) regions, and that of second design has converted to a single (Ag) phase. Shear test results show that the samples are very strong. The breaking forces far exceed requirements in MIL-STD-883 H standards. Fracture incurs inside the joint and is a mix of brittle and ductile modes or only ductile mode. The joint solidus temperatures are 600 °C and 900 °C for the first and second designs, respectively. [DOI: 10.1115/1.4026171]

Keywords: Indium, silver, silver-indium alloys, silver solid solution, high temperature electronics

1 Introduction

In electronic industries, popular die-attach materials are silver-epoxy, lead-free tin-based solders, and gold–tin (Au–Sn) eutectic [1–3]. Among them, the Au–Sn eutectic has the highest operating temperature of 172 °C, which is usually taken at homologous temperature of 0.8. In the advance and market demand of high-temperature electronics, high-temperature device chips built on SiC and GaN-based semiconductors have demonstrated operating temperatures higher than 350 °C. For example, the operating temperature of SiC power devices can go up to 465 °C [4–7]. To assemble these chips on packages, high-temperature die-attachment materials are required. Based upon our literature search, the only thing available is sintered nanosilver paste [8–12]. This new bonding method is gaining ground in applications. In the sintering process, high pressure, such as 10 MPa or higher, is required to consolidate the sintered Ag and reduce pores. Research is being pursued to reduce the sintering pressure and temperature needed.

To produce high-temperature joints at low process temperature, we have studied various binary systems and turned to the silver–indium (Ag–In) binary to design and develop the processes required [13]. For demonstration, we recently bonded 5 mm × 5 mm Si chips to aluminum substrates using fluxless Ag–In design [14]. The bonding was performed at a low temperature of 180 °C. The resulting joint consists of Ag/(Ag)/Ag₂In/(Ag)/Ag, where (Ag) is the solid solution. The solidus temperature of the joint is limited by the solidus temperature of Ag₂In, which is 600 °C. Of the six samples sheared during shear test, only two broke in the joint and the breaking force is 75 kg and 94 kg, respectively. The breakage incurred in the Ag₂In compound layer

and the fracture mode is brittle. The other four broke within Si chips and the actual strength of the joint could not be determined.

Since the Ag₂In compound breaks in brittle mode, in this research, we investigated the possibility of converting the Ag₂In compound layer into (Ag) after the joint is made. Postbonding annealing step is added to convert Ag₂In into (Ag) by continuous reaction with nearby (Ag) and Ag regions. The joint structure of Ag/(Ag)/Ag₂In/(Ag)/Ag is expected to turn into Ag/(Ag)/Ag after the conversion. As a result, the joint solidus temperature will increase from 600 °C to at least 795 °C [13]. Instead of bonding Si chips to Cu substrates, Cu chips are bonded to Cu substrates to ensure that the sample breaks in the joint during shear test. Some preliminary results were recently presented in a conference [15]. In the paper, we report more complete and conclusive analysis and results. In what follows, experimental design and procedures are presented. Experimental results are reported. A summary is then given.

2 Experimental Design and Procedures

Figure 1 depicts the bonding structure design. Cu was chosen to bond to Cu so that the Ag–In joint would break during shear test. For convenience in distinction, the upper Cu is called Cu chip and the bottom one is called Cu substrate. The 12 mm × 12 mm Cu substrates are cut from a 0.8 mm thick Cu sheet having 99.99% purity with mirror finish on one side. The Cu substrates are cleaned thoroughly by rinsing with acetone and de-ionized water to remove contaminations. Ag and In are electroplated sequentially on the Cu substrates. The backside of Cu substrates is painted with lacquer to prevent Ag and In deposition. The Ag plating solution is a cyanide-free, mildly alkaline at pH 10.5. The In plating solution is a sulfamate indium bath at pH 1–3.5. The bath temperature is room temperature for both plating solutions. The current density is 13 mA/cm² for Ag plating and 21.5 mA/cm² for In plating. After plating In layer on the 15 μm Ag layer, a 0.1 μm

¹Corresponding author.

Contributed by the Electronic and Photonic Packaging Division of ASME for publication in the JOURNAL OF ELECTRONIC PACKAGING. Manuscript received July 2, 2013; final manuscript received December 2, 2013; published online January 8, 2014. Assoc. Editor: Yi-Shao Lai.

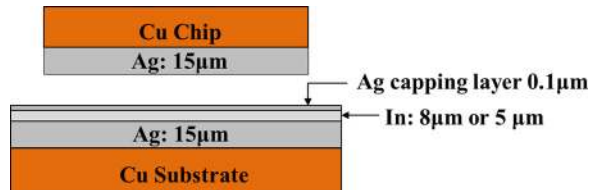


Fig. 1 Bonding structure design of Cu/Ag and Cu/Ag/In/Ag, not to scale. First design: indium thickness = 8 μm , second design: indium thickness = 5 μm .

thin Ag capping layer is plated over the In layer to suppress In oxidation. After plating, the sample is rinsed by de-ionized water and the lacquer on the backside of the Cu substrate is removed by acetone. The 10 mm \times 11 mm Cu chips follow the same cleaning process and are electroplated with a 15 μm Ag layer. The Cu chips and substrates are ready for fluxless bonding experiments. There are two designs, with indium thickness of 5 and 8 μm , respectively. Relatively thick Ag layer of 15 μm is chosen so that the In does not have a chance to reach Cu and react with Cu.

In the fluxless bonding process, the Cu chip is placed over the Cu substrate and held by a fixture with 200 psi static pressure to ensure intimate contact with a silicone buffer [16]. The assembly is mounted on the graphite platform in a vacuum furnace that is pumped to 0.1 Torr to suppress In oxidation during bonding. The

platform is heated and the sample temperature is monitored by a miniature thermal couple. The bonding temperature is set at 180 $^{\circ}\text{C}$ with a dwell time of 6–8 min. The heater is then shut off and the assembly cools naturally in 50 mTorr vacuum. It takes about 90 min to cool to room temperature. No flux is used. After bonding, we annealed the samples at 200 $^{\circ}\text{C}$ for 300, 500, and 1000 h, respectively, to convert the Ag_2In region of the joint to (Ag). A temperature of 200 $^{\circ}\text{C}$ was chosen because it is more compatible with the surviving temperature of most devices. The samples are then cut in cross section to see the quality and compositions of the joints.

To evaluate the quality of the joints, SEM/EDX is employed to determine the chemical compositions, possible intermetallic structure, and microstructures of the samples. Six samples were put through shear tests to evaluate their breaking forces and fracture modes.

3 Experiment Results and Discussions

Two designs were implemented, with In layer thickness of 5 μm and 8 μm , respectively, shown in Fig. 1. We started with In layer thickness of 8 μm , which is thus designated as the first design. When In is plated over Ag, it reacts with Ag to form AgIn_2 compound even at room temperature [17–19]. According to the Ag–In phase diagram in Fig. 2, as temperature increases toward 180 $^{\circ}\text{C}$, the In layer melts at 156 $^{\circ}\text{C}$ and AgIn_2 decomposes

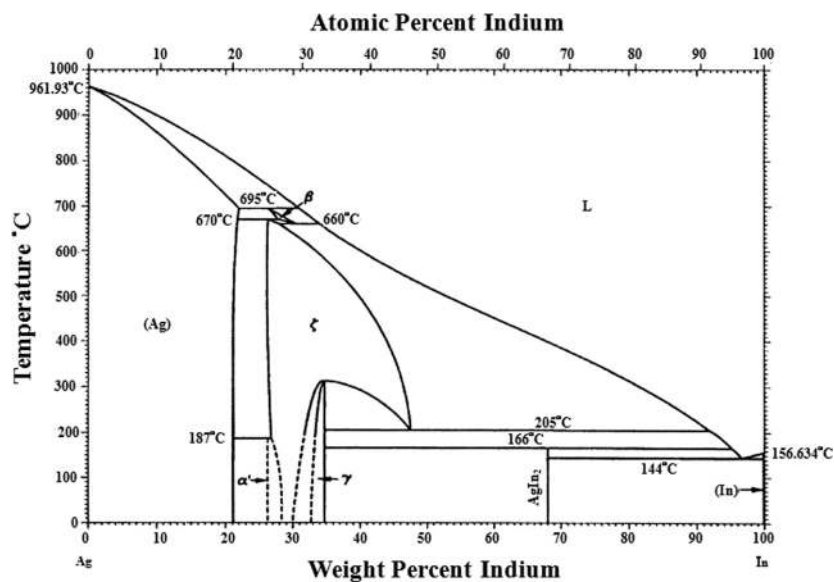


Fig. 2 Silver–indium (Ag–In) binary phase diagram

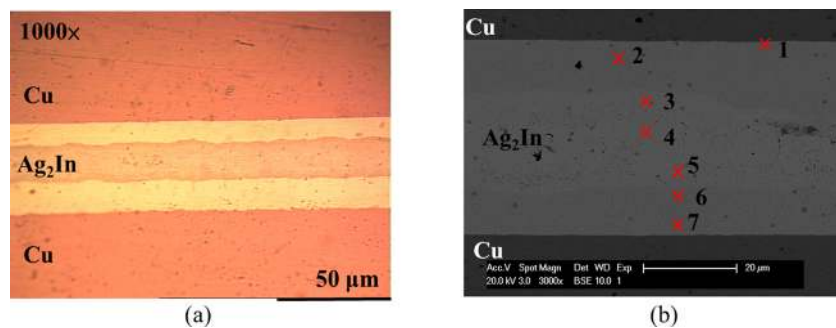


Fig. 3 Cross section optical microscopy image and backscattered SEM image of sample bonded at 180 $^{\circ}\text{C}$. (a) Unannealed, (b) EDX data of layers marked “1”–“7”, and the results are given in Table 1.

Table 1 EDX data on cross section of the sample of first design shown in Fig. 3(b)

Layer on Fig. 3(b)	Composition (at. %)	Corresponding phase
1	Ag: 100, In: 0.00	Ag
2	Ag: 99.62, In: 0.38	(Ag)
3	Ag: 65.99, In: 34.01	Ag ₂ In
4	Ag: 67.27, In: 32.73	Ag ₂ In
5	Ag: 68.47, In: 31.53	Ag ₂ In
6	Ag: 86.08, In: 13.92	(Ag)
7	Ag: 98.48, In: 1.52	(Ag)

into Ag₂In and (In) at 166 °C, where (In) is the indium-rich molten phase [13]. The (In) phase wets and reacts with the Ag layer on the Cu chip to form Ag₂In. When this happens, bonding is essentially achieved. The (In) phase continues to react with both Ag layers to form more Ag₂In until the entire (In) phase is consumed. At this moment, the joint solidifies even at the 180 °C bonding temperature because Ag₂In does not melt until temperature reaches 600 °C [13].

Figure 3(a) displays the cross section optical microscopy (OM) image of a typical bonded sample before annealing at 200 °C. It clearly shows that the sample is well bonded without visible voids. The reddish region is the Ag₂In layer of the joint. A

cross section backscattered SEM image is exhibited in Fig. 3(b). The lighter gray region is the Ag₂In layer, as confirmed by EDX. This Ag₂In region matches that in the OM image. Figure 3(b) also provides the EDX analysis with seven locations marked “1”–“7.” The results are presented in Table 1. Three phases are clearly observed: Ag, (Ag), and Ag₂In. Here, the Ag₂In layer is 15 μm in thickness. It is interesting to note that (ζ) phase, where “Ag₃In” on its Ag-rich boundary is not detected even though it is presented in the phase diagram, Fig. 2.

To convert the Ag₂In region in the joint to (Ag), more samples were produced using the same bonding conditions. These samples were followed by annealing in an oven at 200 °C for 300 h. Figure 4(a) exhibits the cross section OM image of a sample taken from the batch. Slight reddish zone still shows up, indicating that Ag₂In is still in the joint. Figure 4(b) shows the SEM image of the joint with seven locations marked, where EDX data are presented in Table 2. Only three phases, (Ag), (ζ), and Ag₂In, were identified. Pure Ag was not there anymore. Locations 2 and 5 are thought to be (ζ) based on the composition and the phase diagram. To achieve complete conversion of Ag₂In into (Ag), the remaining samples were annealed at 200 °C for additional 200 h for a total annealing time of 500 h. Figure 4(c) exhibits the cross-section OM image of a sample. The slight reddish Ag₂In zone is still in the joint. Figure 4(d) displays the cross section SEM image. EDX analysis indicates that the joint consists of only (Ag)

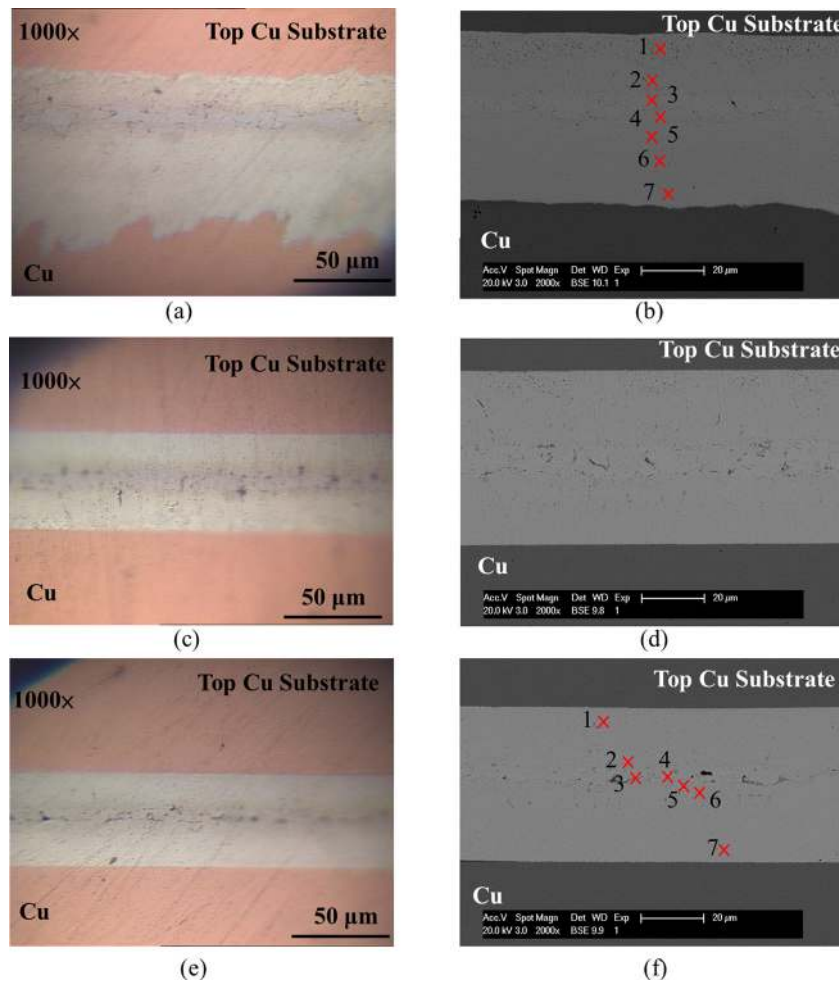


Fig. 4 Cross section OM images and backscattered SEM images of first-design samples bonded at 180 °C. (a) After annealing at 200 °C for 300 h, (b) EDX data of layers shown in (a) marked “1”–“7” and the results are given in Table 2, (c) after annealing at 200 °C for 500 h, (d) cross section backscattered SEM image of the sample shown in (c), (e) after annealing at 200 °C for 1000 h, and (f) EDX data of layers shown in (e) marked “1”–“7” and the results are given in Table 3.

Table 2 EDX data on cross section of the sample of first design shown in Fig. 4(b)

Layer on Fig. 4(b)	Composition (at. %)	Corresponding phase
1	Ag: 91.55, In: 9.45	(Ag)
2	Ag: 74.05, In: 25.95	(ζ)
3	Ag: 70.69, In: 29.31	Ag ₂ In
4	Ag: 66.1, In: 33.90	Ag ₂ In
5	Ag: 76.36, In: 23.64	(ζ)
6	Ag: 84.74, In: 15.26	(Ag)
7	Ag: 90.39, In: 9.61	(Ag)

Table 3 EDX data on cross section of the sample of first design shown in Fig. 4(f)

Layer on Fig. 4(f)	Composition (at. %)	Corresponding phase
1	Ag: 90.81, In: 9.19	(Ag)
2	Ag: 83.63, In: 16.37	(Ag)
3	Ag: 81.22, In: 18.78	(Ag)
4	Ag: 76.78, In: 23.22	(ζ)
5	Ag: 70.88, In: 29.12	Ag ₂ In
6	Ag: 86.15, In: 13.85	(Ag)
7	Ag: 94.86, In: 5.14	(Ag)

with possible small patches of (ζ). The remaining samples were annealed at 200 °C for additional 500 h for a total annealing time of 1000 h. Figure 4(e) shows the cross section OM image of a sample. The slightly reddish Ag₂In region is still in the joint. Figure 4(f) displays the cross section SEM image with locations marked for EDX analysis and results are presented in Table 3. Small patches of Ag₂In and (ζ) are detected in the joint. According to the Ag–In phase diagram, the solidus temperature of the joint is 600 °C which is limited by the Ag₂In phase. After this severe annealing at 200 °C for 1000 h, the samples are still strongly bonded. Shear test results will be reported shortly. Samples bonded with other materials except sintered silver are likely to have failed after this annealing condition [11].

To convert the Ag₂In region of the joint to (Ag) completely, the second design was initiated and implemented, as indicated in Fig. 1. The In thickness is reduced from 8 μm to 5 μm and the Ag thickness has no change. Thinner indium layer results in thinner Ag₂In. This increases the silver composition gradient from silver layers toward Ag₂In region and thus enhances the diffusion rate. The annealing condition was raised from 200 °C to 250 °C to shorten the annealing time. Bonded samples were annealed at several annealing times and studied to examine complete conversion of Ag₂In into (Ag). Figure 5(a) shows the cross section OM image

of a sample after annealing at 250 °C for 350 h. The joint is still bonded well between the Cu chip and Cu substrate. The reddish zone associated with Ag₂In is gone, suggesting complete Ag₂In to (Ag) conversion. Figure 5(b) exhibits the cross section SEM image of the sample, where high quality joint is clearly observed. In Fig. 5(b), the EDX analysis was also performed with 10 locations marked “1”–“10.” These results are presented in Table 4. All locations measured exhibit the composition of (Ag). The annealing process has successfully converted the Ag₂In region of the joint into (Ag). As the result, the joint has only one phase, i.e., (Ag). The Ag composition in (Ag) is higher than 94 at. %. According to the Ag–In phase diagram, the solidus temperature of this (Ag) is 900 °C. It is worth mentioning that samples bonded with other die-attach materials except sintered silver could not have survived this annealing process [11].

The shear test experiment is now presented. Six samples from the first design, i.e., 8 μm In, annealed at 200 °C for 1000 h and seven samples from the second design, i.e., 5 μm In, annealed for 350 h at 250 °C were fabricated for shear testing. For the first-design samples, the sample was mounted on the stage. A tool wedge pushed 10 mm-wide edge of the Cu chip of the sample at a constant speed of 350 μm/s [20]. Figure 6 lists the breaking force and fracture mode. The breaking force ranges from 178 to 200+ kg. Two samples did not break at a force of 200 kg which is the maximum force available from the shear tester. According to military standards MIL-STD-883H method 2019.8, a breaking force higher than 5 kg passes the die shear test. Thus, all six samples far exceed the requirement specified in MIL-STD-883H. Figure 7(a) displays the SEM image of the fracture surface after shear test. The fracture appears to be a mixture of brittle and ductile modes. Quantitative fracture evaluation is underway by tensile test of bulk samples.

For the second design, the samples were sent to Tianjin University (Tianjin Key Laboratory of Advanced Joining Technology and School of Material Science and Engineering, Tianjin University, Tianjin, China) for shear test because the tester over there can better handle the shape of our samples. Figure 6 presents the testing results. The breaking force ranges from 61 to 165 kg. According to military standards MIL-STD-883H method 2019.8, the breaking force of all samples far exceeds the requirement specified in MIL-STD-883H. Figure 7(b) shows the SEM image of the fracture surface. The fracture also appears to be a mixture of brittle and ductile modes. Quantitative fracture evaluation is also underway using tensile test.

It is worth pointing out that the breaking force of the first-design samples is significantly higher than that of the second-design samples (Fig. 6). The joint of the first-design sample consists of mostly (Ag) phase with small regions of (ζ) and Ag₂In compound. Thus, the joint is an alloy of three phases. The joint of

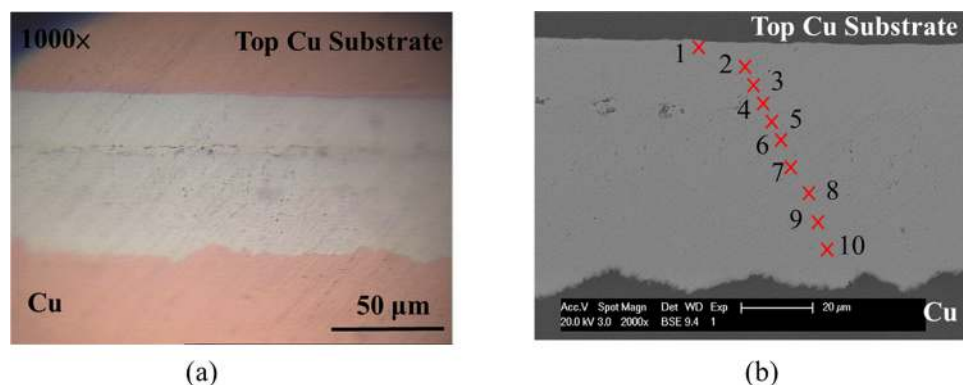


Fig. 5 Cross section OM image and backscattered SEM image of second-design sample bonded at 180 °C. (a) After annealing at 250 °C for 350 h, (b) EDX data of layers marked “1”–“10”, and the results are given in Table 4.

Table 4 EDX data on cross section of the sample of second design shown in Fig. 5(b)

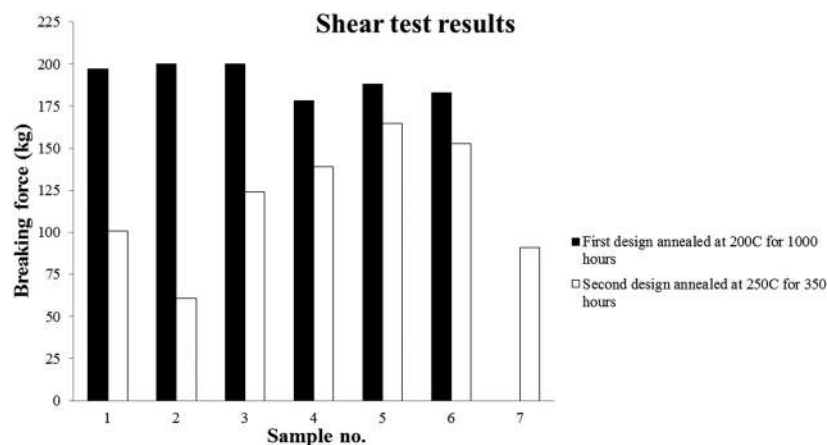
Layer on Fig. 5(b)	Composition (at. %)	Corresponding phase
1	Ag: 96.38, In: 3.62	(Ag)
2	Ag: 96.09, In: 3.91	(Ag)
3	Ag: 95.69, In: 4.31	(Ag)
4	Ag: 94.78, In: 5.22	(Ag)
5	Ag: 94.18, In: 5.82	(Ag)
6	Ag: 94.53, In: 5.47	(Ag)
7	Ag: 95.70, In: 4.30	(Ag)
8	Ag: 94.60, In: 5.40	(Ag)
9	Ag: 96.43, In: 3.57	(Ag)
10	Ag: 97.21, In: 2.79	(Ag)

the second-design samples consists of only the (Ag) phase. The breaking force data seem to suggest that an alloy joint is stronger than a single (Ag) phase joint. This is a preliminary assessment. Further investigation is required to confirm it.

4 Summary

Advances in semiconductor technology have demonstrated device chips that achieve operation temperature as high as 465 °C [4–7]. To put these chips into operations, they have to be bonded to a substrate or package and wired. The resulting joint must have high enough solidus temperature. Among all common die-attach materials, only sintered nanosilver and Au–Sn alloys with Au composition higher than 85 wt. % can meet this aim.

In this research, we looked into the Ag–In system and developed fluxless low-temperature processes to produce high-strength and high-temperature joints between two Cu substrates. After



First design annealed at 200°C for 1000 hours	1	2	3	4	5	6	
Breaking force (kg)	197	200+	200+	178	188	183	
Fracture mode	Ag-In joint	No breakage		Ag-In joint			
Second design annealed at 250°C for 350 hours	1	2	3	4	5	6	7
Breaking force (kg)	101	61	124	139	165	153	91
Fracture mode	Ag-In joint						

Fig. 6 The bar chart and table illustrate the breaking forces of the six samples of the first design annealed at 200 °C for 1000 h and seven samples of the second design annealed at 250 °C for 350 h. The shear tester could not break samples 2 and 3 of first design.

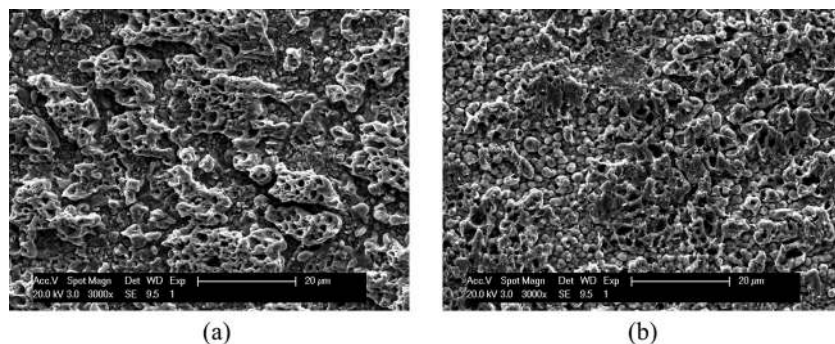


Fig. 7 SEM image of the fracture surface of samples after the shear test. (a) First-design sample: EDX detects Ag_2In , In , and (Ag) and (b) second-design sample: EDX detects only the solid solution phase (Ag) .

bonding at 180 °C, the samples were annealed at 200–250 °C to alter the compositions and microstructures to increase the solidus temperature, the strength, and ductility. Two designs were experimented with. For the first design, the samples were annealed at 200 °C for 1000 h. The joint solidus temperature is at least 600 °C. Of the six samples sheared, the breaking force ranges from 178 kg to 200+ kg. The shear tester could not break two of the six samples. These results far exceed the 5 kg requirement in military standards MIL-STD-883H method 2019.8. The fracture incurs inside the joint. The joint structure is an alloy of mostly (Ag) solid solution embedded with micron-size (ζ) and Ag_2In regions. For the second design, the samples were annealed at 250 °C for 350 h. Seven samples were sheared and the breaking force ranges from 61 to 165 kg which far exceeds the requirement in military standards. Fracture also incurs inside the joint. The joint consists of only (Ag) phase with Ag composition higher than 94 wt. %. The solidus temperature is 900 °C. For either design, the samples break in a mix of brittle and ductile modes or ductile mode only.

The research results have shown that high-strength and high-temperature joints can be manufactured using fluxless low-temperature processes with the Ag–In system. Compared with the Au-rich Au–Sn alloy bonding technique that results in Au composition between 90 and 95 wt. %, this method is much more affordable because the price of Au is 60 times of Ag. Compared with sintered nanosilver technique, this method is less expensive because the manufacturing cost of nanosilver paste is very high, about 5× of Ag cost. One gram of nanosilver paste in production quantity costs 5× of the market value of Ag. Accordingly, the technology reported here should be valuable in developing high-temperature packages.

Acknowledgment

The authors greatly appreciated the support and encouragement from II-VI Foundation. They also thank Professors Guo-Quan Lu and Xu Chen, Dr. Gang Chen and Dr. Yunhui Mei, and their students Yunjiao Cao and Dan Han of Tianjin Key Laboratory of Advanced Joining Technology and School of Material Science and Engineering, Tianjin University, China, for performing the shear test of the second-design samples.

References

- [1] Pecht, M. G., Agarwal, R., McCluskey, P., Dishongh, T., Javadpour, S., and Mahajan, R., 1998, "Zeroth-Level Packaging Materials," *Electronic Packaging: Materials and Their Properties* (Electronic Packaging Series), M. G. Pecht, ed., CRC Press LLC, Boca Raton, FL, pp. 25–28.

- [2] Puttlitz, K. J., 2004, "Overview of Lead-Free Solder Issues Including Selection," *Handbook of Lead-Free Solder Technology for Microelectronic Assemblies*, K. J. Puttlitz and K. A. Stalter, eds., Marcel Dekker, Inc., New York, pp. 1–48.
- [3] Bjorneklett, A., Halbo, L., and Kristiansen, H., 1992, "Thermal Conductivity of Epoxy Adhesives Filled With Silver Particles," *Int. J. Adhes. Adhes.*, **12**(2), pp. 99–104.
- [4] Pyo, S., and Sheng, K., 2009, "Junction Temperature Dynamics of Power MOSFET and SiC Diode," *IEEE 6th International Power Electronic and Motion Control Conference*, Wuhan, China, May 17–20, pp. 269–273.
- [5] Cao, X. A., Van Hove, J. M., Klaassen, J. J., Polley, C. J., Wowchack, A. M., Chow, P. P., King, D. J., Ren, F., Dang, G., Zhang, A. P., Abernathy, C. R., and Pearton, S. J., 2000, "High Temperature Characteristics of GaN-Based Heterojunction Bipolar Transistors and Bipolar Junction Transistors," *Solid-State Electron.*, **44**(4), pp. 649–654.
- [6] Manikam, V. R., and Cheong, K. Y., 2001, "Die Attach Materials for High Temperature Applications: A Review," *IEEE Trans. Compon., Packag., Manuf. Technol.*, **1**(4), pp. 457–478.
- [7] Chin, H. S., Cheong, K. Y., and Ismail, A. B., 2010, "A Review on Die Attach Materials for SiC-Based High-Temperature Power Devices," *Metall. Mater. Trans. B*, **41B**(4), pp. 824–832.
- [8] Wang, T., Chen, X., Lu, G. Q., and Lei, G. Y., 2007, "Low-Temperature Sintering With Nano-Silver Paste in Die-Attached Interconnection," *J. Electron. Mater.*, **36**(10), pp. 1333–1340.
- [9] Bai, J. G., Lei, T. G., Calata, J. N., and Lu, G. Q., 2007, "Control of Nanosilver Sintering Attained Through Organic Binder Burnout," *J. Mater. Res.*, **22**(12), pp. 3494–3500.
- [10] Ning, P., Lei, T. G., Wang, F., Lu, G. Q., and Ngo, K. D. T., 2010, "A Novel High-Temperature Planar Package for SiC Multichip Phase-Leg Power Module," *IEEE Trans. Power Electron.*, **25**(8), pp. 2059–2067.
- [11] Knoerr, M., Kraft, S., and Schletz, A., 2010, "Reliability Assessment of Sintered Nano-Silver Die Attachment for Power Semiconductors," *IEEE 12th Electronic Package Technology Conference (EPTC)*, Singapore, December 8–10, pp. 56–61.
- [12] Kuramoto, M., Ogawa, S., Niwa, M., Kim, K. S., and Suganuma, K., 2011, "New Silver Paste for Die-Attaching Ceramic Light-Emitting Diode Packages," *IEEE Trans. Compon., Packag. Manuf. Technol.*, **1**(5), pp. 653–659.
- [13] Okamoto, H., and Massalski, T. B., eds., 1990, "Ag–In (Silver–Indium)," *Binary Alloy Phase Diagrams*, ASM International, Metal Park, OH, pp. 47–48.
- [14] Wu, Y. Y., and Lee, C. C., 2013, "Bonding Silicon Chips to Aluminum Substrates Using Ag–In System Without Flux," *IEEE Trans. Compon., Packag. Manuf. Technol.*, **3**(5), pp. 711–715.
- [15] Wu, Y. Y., and Lee, C. C., 2013, "Growth and Strength of the Solid Solution Phase (Ag) With Indium," *IEEE 63rd Electronic Components and Technology Conference (ECTC)*, Las Vegas, NV, May 28–31, pp. 1783–1787.
- [16] Lee, C. C., Wang, D. T., and Choi, W. S., 2006, "Design and Construction of a Compact Vacuum Furnace for Scientific Research," *Rev. Sci. Instrum.*, **77**(12), p. 125104.
- [17] Wang, P. J., Kim, J. S., and Lee, C. C., 2009, "Intermetallic Reaction of Indium and Silver in an Electroplating Process," *J. Electron. Mater.*, **38**(9), pp. 1860–1865.
- [18] Gollas, B., Albering, J. H., Schmut, K., Pointner, V., Herber, R., and Eitzkom, J., 2008, "Thin Layer In Situ XRD of Electrodeposited Ag/Sn and Ag/In for Low-Temperature Isothermal Diffusion Soldering," *Intermetallics*, **16**(8), pp. 962–968.
- [19] Roy, R., and Sen, S. K., 1992, "The Kinetics of Formation of Intermetallics in Ag/In Thin Film Couples," *Thin Solid Films*, **197**(1–2), pp. 303–318.
- [20] SMTnet, 2010, Surface Mount Technology Industry Directory; Nordson DAGE, Fremont, CA, http://www.smtnet.com/company/index.cfm?fuseaction=view_company&company_id=48999